Catalysis Science & Technology

PAPER

Cite this: *Catal. Sci. Technol.*, 2016, **6**, 6320

Carbonyl group-dependent high-throughput screening and enzymatic characterization of diaromatic ketone reductase†

Jieyu Zhou, Guochao Xu, Ruizhi Han, Jinjun Dong, Weiguo Zhang, Rongzhen Zhang and Ye Ni*

Received 27th April 2016,
Accepted 20th May 2016

DOI: 10.1039/c6cy00922k

www.rsc.org/catalysis

We have developed a carbonyl group-dependent colorimetric method for assay of carbonyl reductases using inexpensive 2,4-dinitrophenylhydrazine (DNPH). This DNPH method has high sensitivity and low background disturbance, and can be used for high-throughput screening of carbonyl reductases toward various ketones including diaromatic ketones, aliphatic ketones/diketones, and aromatic ketones. For 1-(4′-chlorophenyl)-1-(pyridine-2′-yl)-methyl ketone (CPMK), a characteristic absorbance peak at around 500 nm was observed for the product of CPMK and DNPH with a molar absorbance coefficient of 13 750 L mol^{-1} cm^{-1}. Significantly, this method is also amendable to whole-cell systems for facile high-throughput screening and substrate specificity profiling. In random mutagenesis of a diaromatic ketone reductase *Kp*ADH, three variants (M131F, S196Y and S237A) with improved activity toward CPMK were identified using the DNPH method. The substrate specificity of *Kp*ADH and its variants toward sixteen prochiral ketones was well characterized. Furthermore, kinetics and molecular docking analyses of *Kp*ADH and its variants were performed to elucidate the potential catalytic and enantioselective mechanisms. Consequently, our study provides a rapid screening and characterization method for carbonyl reductases with potential applications in the preparation of optically active secondary alcohols.

Introduction

Asymmetric reduction of ketones is one of the most important methods for the synthesis of optically active secondary alcohols, especially diaromatic alcohols, which are vital building blocks of pharmaceuticals, agrochemical, flavors, *etc.*[1,2] Biocatalytic reduction of prochiral ketones using carbonyl reductases is regarded as a viable "green" alternative due to its high enantioselectivity, environmental compatibility, and mild reaction conditions.[3,4] There is a constant need for novel carbonyl reductases with expected properties, such as high activity, enantioselectivity and stability.[5]

The development of novel carbonyl reductases with desired functions has been boosted with advances in genomic data, protein expression and molecular engineering technologies; however it was limited by the availability of new reductases identified through activity and substrate profile screening.[6] Sensitive, facile and efficient high-throughput methods have become essential for the identification and engineering of reductases.[7] The most accurate methods for the determination of reductase activity are GC/HPLC, providing an evaluation of conversion and stereoselectivity simultaneously; however they are usually time-consuming and have a low throughput. Well established high-throughput screening (HTS) methods are based on the characteristic absorbance of NAD(P)H and the chromogenic reaction on specific groups of the substrate/product, since the substrates/products are generally colorless or non-fluorescent (Table 1).[8,9] Although various reductases have been engineered using HTS based on NAD(P)H,[10] the high cost of NAD(P)H, high noise disturbance of background expression and inapplicability in whole-cell systems are the main obstacles. Additionally, the accuracy of NAD(P)H measurement is dependent on certain concentrations due to its low molar absorbance coefficient. He and coworkers established a screening method for β-keto esters reductase using acidic ferric perchlorate which could form a purple ferric compound with the enol group of β-keto esters.[11] However, the procedure was cumbersome when operating in 96-well plates since the unreacted β-keto esters must be extracted from the reaction mixture by ethyl acetate for chromogenic reaction. Forchin and coworkers developed a HTS method for ene-reductase based on the assay of

The Key Laboratory of Industrial Biotechnology, Ministry of Education, School of Biotechnology, Jiangnan University, Wuxi 214122, Jiangsu, China.
E-mail: yni@jiangnan.edu.cn

† Electronic supplementary information (ESI) available. See DOI: 10.1039/c6cy00922k

Table 1 Comparison of high-throughput screening methods for carbonyl reductases

Entry	Reagent	Molar absorbance coefficient/wavelength [L mol^{-1} cm^{-1}]/[nm]	Time [min]	Advantage	Disadvantage	Ref.
1	NAD(P)H	6220/340	5	Applicability to all prochiral ketones	Low molar absorbance coefficient, dependent on high price NAD(P)H, not suitable in whole cell systems	10
2	NBT–PMS[a]	n.a.[c]/560	30	Colony screening	Dependent on high price NAD(P)H	8
3	$Fe(ClO_4)_2$	n.a./510	30	Whole cell systems	Only suitable to β-ketoesters	11
4	GOx[b]/Peroxidase	n.a./500	20	Applicability in glucose dependent systems and biphasic systems	High background interference, only applied in crude enzyme systems	12
5	DNPHzine	13 750/500	30	High sensitivity and applicability in whole cell systems	Unsuitable to ketoesters	This work

[a] NBT–PMS: nitroblue tetrazolium/phenazine methosulfate. [b] GOx: glucose oxidase. [c] n.a.: not available.

glucose consumed in cofactor regeneration using glucose oxidase and peroxidase.[12] However, this HTS method could be easily disturbed by the background glucose consumption, and is strictly restricted to purified enzyme systems.

As widely accepted, the library size is crucial for random or semi-rational mutagenesis to obtain desirable mutants.[13] An easily operated and whole-cell system adaptable method is advantageous for fast identification and characterization of vast amounts of variants with versatile properties. Herein we present a facile and inexpensive high-throughput method for the screening and characterization of reductases toward prochiral ketone substrates. The formation of chromogenic products in the reaction between ketone/aldehyde groups and 2,4-dinitrophenylhydrazine (DNPHzine) under basic conditions is well-known, and has been recorded far back in the early 20th century in the identification of aldehydes and ketones.[14] The produced 2,4-dinitrophenylhydrozone (DNPHzone) is orange (or red-brown) and sensitive in the assay even at trace amounts in fermentation broth, foodstuff or air samples.[15,16] Xue and coworkers successfully employed DNPHzine in the screening of dehydrogenase with high enantioselectivity in the oxidative resolution of (*R*)- and (*S*)-α-hydroxyacid into α-ketoacid.[17] An efficient method using fluorimetric 7-hydrazino-4-nitrobenzo-2,1,3-oxadiazole (NBDH) was developed to form highly fluorescent derivatives *via* hydrazine formation with carbonyl groups in proteins, and as low as 0.2 nmol mg^{-1} protein carbonyls could be detected with a precision of 5%.[18] We thus proposed to use this DNPHzine in the high-throughput screening of carbonyl reductase and profiling of substrate specificity toward various prochiral ketones (Scheme 1). Optimizations were performed to simplify the procedures for much more facile and sensitive screening and characterization of carbonyl reductases, especially in the whole-cell system. Previously, we have identified a diaromatic ketone reductase, *Kp*ADH, from *Kluyveromyces polyspora* (GenBank accession no. EDO16647.1), however with relatively low activity (0.118 U mg^{-1} wet cells) and moderate enantioselectivity (82.0% (*R*)). Hence we investigated the potential of this DNPH method in the engineering of *Kp*ADH.

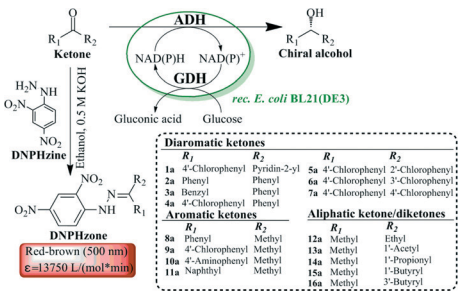

Scheme 1 High-throughput colorimetric method for determining the activities of carbonyl reductases toward various prochiral ketones.

Experimental section

Plasmid, strains and reagent

Recombinant pET28-*Kp*ADH, *E. coli* BL21(DE3)/pET28-*Kp*ADH and *E. coli* BL21(DE3)/pET28-GDH, were constructed as previously described.[19] (4-Chlorophenyl)-(pyridin-2-yl)methanone (CPMK, **1a**), all other reagents, analytical grade solvents and biochemical reagents were obtained from Sinopharm Chemical Reagent Co. Ltd.

Establishment of DNPH method

To establish a high-throughput screening method in 96-well plates, the reaction system should be easily operated in small volumes. The reaction composition and various conditions were optimized. General reductive reaction consisted of 40 μL of enzyme solution, 20 μL of CPMK (25 mM), 20 μL of glucose (50 mM) and 20 μL of glucose dehydrogenase solution (100 μL in total). The reaction mixture was shaken at 30 °C and 120 rpm for 40 min. General chromogenic reaction was performed by addition of 100 μL of DNPH (20 mM, dissolved in ethanol containing 3% sulfuric acid) into 100 μL of the above mentioned reaction mixture and standing for 30 min at 30 °C. And then 1 mL of KOH (0.5 M) was added, and the absorbance of the red-brown solution in the plates was determined at 500 nm by an absorbance microplate reader

(Biotek, USA). The effect of incubation time and alkali was determined according to the general methods except for the different incubation times (10 min, 20 min, 30 min, 1 h and 2 h), alkalis (NaOH, KOH, $NaHCO_3$, $KHCO_3$, Na_2CO_3 and K_2CO_3) and concentrations (0.5 M and 1.0 M) to achieve high sensitivity.

Standard curve of CPMK using DNPH method

Different concentrations of **1a** (0.25–3.0 mM) were mixed with 20 μL of glucose (50 mM) and 20 μL of glucose dehydrogenase solution (100 μL in total), and shaken at 30 °C and 120 rpm for 40 min. Afterwards, the absorbance was determined by the general chromogenic reaction method.

Pearson correlation coefficient analysis and recovery rate

The Pearson correlation coefficient was analyzed by comparing the same CPMK concentration determined by DNPH and HPLC methods. Various concentrations of CPMK (0.25–3.0 mM) were assayed by the DNPH method as mentioned above and also determined using an Agilent 1100 HPLC equipped with a Chiralcel OB-H column (0.46 mm × 250 mm, 5 μm, Diacel, Japan). HPLC was performed at 254 nm using hexane : ethanol (95 : 5, v/v) as eluent at a flow rate of 1.0 mL min^{-1} and 30 °C.

Recovery rate experiments were performed to test the reliability of this DNPH method. The CPMK concentration in the initial sample is 0.88 mM. Then different volumes of 5 mM CPMK were added into the initial sample, and the actual values of added CPMK concentrations were 0.044, 0.088 and 0.132 mM, respectively. The concentrations of these mixed samples were determined using the DNPH method. Theoretically, the concentration difference between the mixed samples and initial sample should equal the actual values of added CPMK concentrations. The recovery rate was calculated according to the following formula.

$$\text{Recovery rate}\ (\%) = \frac{[\text{Mixed CPMK}] - [\text{Initial CPMK}]}{[\text{Added CPMK}]} \times 100\%$$

Standard curves of various prochiral ketones using DNPH method

Standard curves of prochiral ketones (**1a–16a**) with various concentrations (0–2.0 mM) were determined by the DNPH method.

General protocol for protein expression

Recombinant *Kp*ADH were prepared by cultivation of *E. coli* BL21(DE3) harboring pET28-*Kp*ADH at 37 °C and 180 rpm in LB medium supplemented with 50 μg mL^{-1} kanamycin. Until the OD_{600} reached 0.6–0.8, 0.2 mM isopropyl-β-D-thiogalactopyraniside was added and further cultured at 25 °C. After induction for 12 h, the cells were harvested by centrifugation (8000 × *g*, 10 min) and disrupted by a high-pressure homogenizer (ATS BASIC-II, ATS ENGINEERING Inc., Shanghai) or directly lyophilized under vacuum (SCIENTZ-10N, NINGBO SCIENTZ BIOTECHNOLOGY Co., Ltd., Ningbo) to prepare dry cells of *Kp*ADH, and stored at 4 °C for further use. Recombinant *Kp*ADH and variants were purified to homogeneity as previously described.[19]

Conversion of CPMK using *Kp*ADH

The asymmetric reduction of CPMK was conducted with 7.5 mM **1a**, 1.0 g L^{-1} *Kp*ADH, 20 mM glucose, and 100 μL of glucose dehydrogenase solution (10 mL in total) at 30 °C and 180 rpm. About 20 μL of the sample was withdrawn from the reaction mixture and measured by the DNPH method. The conversion of **1a** was also determined using the Agilent 1100 HPLC equipped with a Chiralcel OB-H column (0.46 mm × 250 mm, 5 μm, Diacel, Japan). HPLC was performed at 254 nm using hexane : ethanol (95 : 5, v/v) as eluent at a flow rate of 1.0 mL min^{-1} and 30 °C. Conversion of **1a** using different amounts of *E. coli* BL21 harboring pET28-*Kp*ADH and *E. coli* harboring empty pET28a whole cells was carried out with 0.5 mM **1a** and different amounts of whole cells (10, 20 and 30 mg DCW). Reactions were conducted, and samples were withdrawn and prepared as mentioned above.

Error prone PCR, library construction and cultivation

Error-prone PCR of *Kp*ADH (GenBank accession no. EDO16647.1) was performed using recombinant plasmid pET28-*Kp*ADH as a template. Error-prone PCR was carried out using a PCR thermal cycler (BIORAD, USA). A 25 μl reaction mixture contains 10× reaction buffer, 2.5 mM dNTP mix, 100 μM $MnSO_4$, 500 μM $MgCl_2$, 0.16 μM of each primer pair, 10 ng of the template, and 1.25 U rTaq polymerase (TaKaRa, Japan) in ultra-pure water. Primers were *Kp*ADH-forward (5′-TGGGTCGCGGATCCGAATTCATGAGCGTATTAATTAGTGGTGCTTC-3′) and *Kp*ADH-reverse (5′-GTGGTGGTGGTGGTGCTCGAGAACTCTA CCTTCTTTATGTAAAATTTGATAGA-3′). PCR was carried out at 95 °C for 30 s, 54 °C for 30 s, and 72 °C for 90 s for a total of 30 cycles. Afterwards, the resultant PCR products were inserted into the pET28a vector between *Eco*RI and *Xho*I sites using Exnase MultiS (Vazyme, Nanjing, China), followed by transformation into *E. coli* BL21(DE3). The recombinant cells were spread on LB plates supplemented with 50 μg mL^{-1} kanamycin (Kan) and incubated at 37 °C overnight to form the library.

Colonies on LB plates were picked up and transferred into 96-deep well plates (each well containing 300 μL of LB medium and 50 μg mL^{-1} Kan). After cultivation at 37 °C for 6 h, 50 μL of the culture was transferred into new 96-deep well plates (each well containing 450 μL of LB medium and 50 μg mL^{-1} Kan). After further cultivation for 2 h at 37 °C, 0.2 mM isopropyl β-D-1-thiogalactopyranoside (IPTG) was added to induce expression of *Kp*ADH at 30 °C, 120 rpm for 4 h, and then the cells were harvested by centrifugation (4000*g* for 10 min).

High-throughput screening of the random mutagenesis library

The harvested cells were resuspended in 40 μL of phosphate buffer (100 mM, pH 7.0) and screened using the general reductive method. The mixtures were shaken at 30 °C and 120 rpm for 40 min, then 100 μL of DNPH (20 mM, dissolved in ethanol containing 3% sulfuric acid) and 1.0 mL of KOH (0.5 M) were added for colorimetric reaction according to the general chromogenic reaction method. One unit of the activity (U) was defined as the amount of wet cells required for catalyzing the reduction of 1 μmol of CPMK per minute. Wells inoculated with *E. coli* BL21(DE3)/pET28-*Kp*ADH were regarded as positive controls, and wells without inoculation were negative controls.

High-throughput characterization of *Kp*ADH and three variants

One-gram wet weight cells of *Kp*ADH and variants (M131F, S196Y and S237 A) were resuspended in 50 mL of phosphate buffer (pH 7.0, 100 mM). Fifty five μL of cell suspension, 10 μL of glucose solution (100 mM) and 20 μL of cell lysis solution of *E. coli* BL21 (DE3)/pET28-GDH were mixed and added into 96-deep well plates. Prochiral ketone solutions (15 μL, 20 or 50 mM, dissolved in ethanol) were added to start the reaction. The mixtures were shaken at 30 °C and 120 rpm for 40 min or 6 h, and controls were prepared without cells or ketones. Then 100 μL of DNPH solution was added into each well and kept static for 30 min at 30 °C. After that, 1 mL of KOH (0.5 M) was added, and the absorbance at 500 nm of each well was determined by a microplate reader (Biotek, USA). All the assays were carried out in triplicate.

Kinetic analysis

The kinetic parameters of the purified *Kp*ADH and variants towards **1a** were measured by determining the activity at different **1a** concentrations (0.1–2.5 mM) and a fixed NADPH concentration (1.0 mM). The apparent K_m and V_{max} values were calculated according to the Lineweaver–Burk plot.[20]

Homology modeling and molecular docking

Homology structures of *Kp*ADH and variants were constructed with EasyModeller v4.0 using the crystal structure of yeast methylglyoxal/isovaleraldehyde reductase (PDB No. 4PVD) as a template.[21] All docking calculations were accomplished with AutoDock Vina 1.1.[22] A docking algorithm that takes account of the ligand flexibility but keeps the protein rigid was employed. Docking runs were carried out using the standard parameters of the program for interactive growing and subsequent scoring, except for the parameters for setting grid box dimensions and center as follows: center_x = 23.567; center_y = 9.975; center_z = 112.348; size_x = 20; size_y = 20; size_z = 20.

Results and discussion

Establishment of the high-throughput DNPH method for reductase

Optically active 1-(4′-chlorophenyl)-1-(pyridine-2′-yl)-methanol (CPMA) is an important chiral intermediate of anti-allergic drugs, which could be synthesized by the asymmetric reduction of CPMK. However, CPMK is a non-natural diaromatic ketone, and could barely be reduced by most reductase. Therefore, CPMK was chosen as the model substrate in the establishment of the DNPH method. Initially, the efficacy of this DNPH method was demonstrated in the determination of reductase activity toward 1-(4′-chlorophenyl)-1-(pyridine-2′-yl)-methyl ketone (CPMK, **1a**), assisted with glucose dehydrogenase for cofactor regeneration. The potential influence of the four components of the reaction system, including **1a**, NADPH, glucose and glucono-δ-lactone, *Kp*ADH and glucose dehydrogenase, were studied, since ketone/aldehyde groups might interact with DNPHzine. The product of **1a** and DNPHzine displays a characteristic absorbance peak at around 500 nm according to the absorbance spectrum (Fig. 1(A)), which is distinct from that of NADPH, glucose, glucono-δ-lactone, recombinant *Kp*ADH and glucose dehydrogenase and *E. coli* BL21(DE3) cells (Fig. S1†). Low disturbance of NADPH, glucose and glucono-δ-lactone was detected, indicating the feasibility of DNPH in the assay of CPMK reductase.

Effects of incubation time and type of base on the colorimetric reaction between DNPHzine and **1a** were studied. As a HTS method, the procedure should be simple and quick. The reaction time between DNPHzine and **1a** was optimized. Thirty minutes of incubation at 30 °C and 180 rpm was proved to be enough for producing DNPHzone, with obvious red-brown color. Red-brown DNPHzone was formed between DNPHzine and ketones in basic solutions, and several alkalis including NaOH, KOH, $NaHCO_3$, $KHCO_3$, Na_2CO_3 and K_2CO_3 with different pK_b values were investigated. However, only NaOH and KOH could produce clear red-brown color (Fig. 1(B)), indicating the positive effect of the hydroxyl group in the colorimetric reaction, and KOH was selected as the chromogenic reagent. Furthermore, 0.5 M KOH was determined to be appropriate in the chromogenic reaction after different concentrations of KOH were evaluated.

The calibration curve and the detection limit of the DNPH method are required for the quantification of **1a** concentration in the bioreduction system. As shown in Fig. S8,† a linear relationship was observed between **1a** concentration and OD_{500} from 0.02 to 0.307 mM, suggesting the feasibility of the DNPH method at low **1a** concentrations. The color becomes dark red-brown along with the increase of **1a** concentration (Fig. 1(B)). The molar absorbance coefficient (ε) is calculated to be 13 750 L mol^{-1} cm^{-1} at 500 nm, which is 1.2 times higher than that of NAD(P)H at 340 nm (6220 L mol^{-1} cm^{-1}, Table 1).[23] The detection limit of the DNPH method was examined according to IUPAC definition.[24] The lowest detection concentration for **1a** is 0.199 mg L^{-1} with a Z-factor of 0.896. All the above results demonstrate that this DNPH

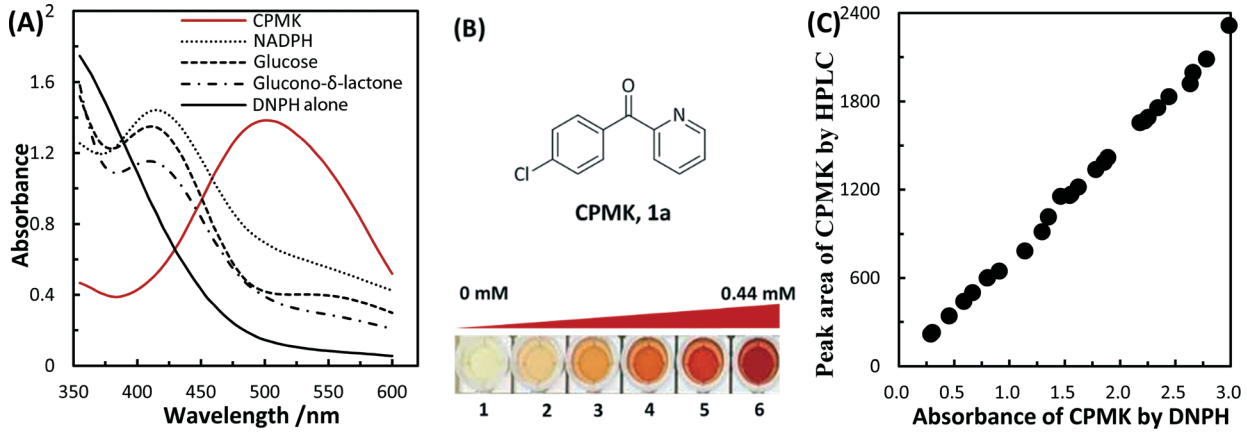

Fig. 1 Absorbance spectra of CPMK, NADPH, glucose and glucono-δ-lactone with DNPHzine, and DNPH alone (A), red-brown color formation between different concentrations (0, 85.5, 177, 265, 354 and 442 μM) of CPMK and DNPHzine (B), and CPMK concentration determined by HPLC and DNPH methods (C).

method is sensitive enough for the quantification of **1a** in the context of enzyme screening.

Afterwards, the reliability of the DNPH method was further evaluated against HPLC analysis, which is regarded as the most precise method for the activity assay. More than thirty samples were measured by both DNPH and HPLC methods as illustrated in Fig. 1(C). The concentration determined by DNPH is highly consistent with that obtained by HPLC. The Pearson correlation coefficient[25] between DNPH and HPLC methods is 0.99. The precision of the DNPH assay was also investigated by recovery rate experiments, which were performed by addition of 0.044, 0.088 and 0.132 mM **1a** into the test samples (Table 2). The recovery rates were calculated to be 102.3%, 102.3% and 103.3%, respectively. Since 95–105% recovery rates are acceptable,[26] the DNPH method is exceptionally reliable and could be adopted in activity assay of carbonyl reductases.

Conversion analysis of the whole cell system

An excellent HTS method should be applicable not only to the isolated enzyme system, but also to the whole-cell system especially for carbonyl reductases which are cofactor-dependent. In asymmetric reduction of 7.5 mM **1a** employing recombinant *E. coli* BL21(DE3) whole cells, the conversion was determined by both HPLC and DNPH methods. The conversion was calculated based on the decrease of **1a**, about 49.1 and 51.6% conversions were determined by DNPH and HPLC methods, respectively. A similar tendency was obtained with these two methods as shown in Fig. 2(A), proving the potential of the DNPH method in the whole-cell bioreductive system. The effect of whole cell amount on the asymmetric reduction of **1a** was optimized (Fig. 2(B)). The initial reaction rate increased with the increase of recombinant whole cells from 10 to 30 mg in the 20 mL reaction mixture loaded with 0.5 mM **1a**. Within 30 min, less than 0.05 mM **1a** was

Table 2 Recovery rate experiments of the DNPH method

Entry	Initial CPMK [mM]	Added CPMK [mM]	Mixed CPMK [mM]	Recovery [%]
1	0.088 ± 0.002	0.044	0.133 ± 0.001	102.3
2	0.088 ± 0.002	0.088	0.178 ± 0.002	102.3
3	0.088 ± 0.002	0.132	0.224 ± 0.001	103.1

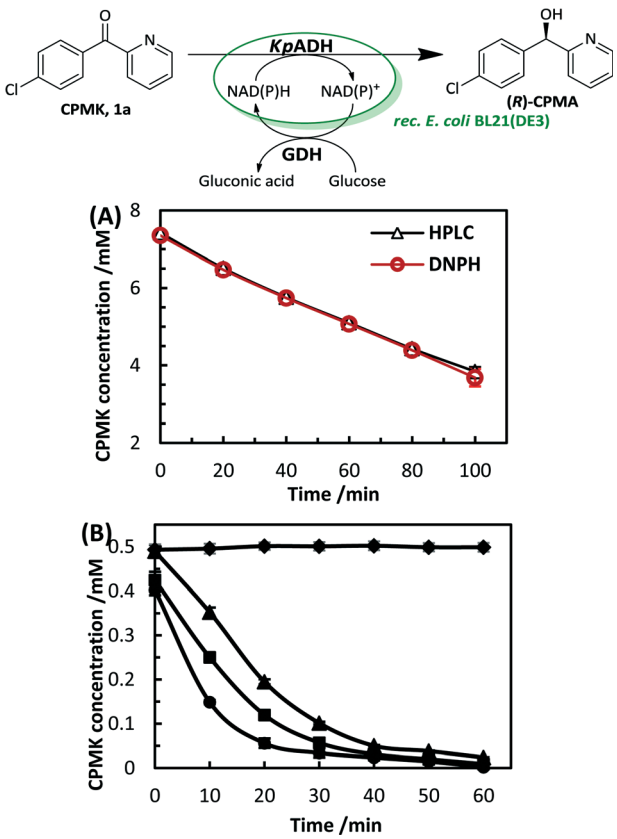

Fig. 2 Time course of the asymmetric reduction of **1a** with *Kp*ADH. (A) Conversion of 7.5 mM **1a** determined by HPLC (Δ) and DNPH (○) methods; (B) the effect of whole cell amount on the reduction of 0.5 mM **1a**, (▲) 10 mg, (■) 20 mg, (●) 30 mg, (♦) 30 mg of *E. coli* cells harboring pET28a.

detected in the reaction mixture employing 30 mg of whole cells (1.5 g L^{-1}). **1a** was completely converted into CPMA in 60 min.

High-throughput screening of *Kp*ADH mutants toward CPMK

The feasibility of this DNPH method in high-throughput screening was also evaluated. To obtain variants with improved activity, a random mutagenesis library of *Kp*ADH containing about 2000 variants was developed and screened using the DNPH high-throughput method (Fig. S2†). The amino acid mutation rate was about 0.5% in average. Most of the variants were inactivated, and about 10% of the variants retained the activity toward **1a** (Fig. 3). Among them, 4% of the variants displayed higher conversion. After sequencing, three variants (*Kp*ADH_{M131F}, *Kp*ADH_{S196Y} and *Kp*ADH_{S237A}) showed the highest conversion. It is commonly understood that the residues playing important roles in activity are mostly located in the substrate binding pocket.[27] Residues M131, S196 and S237 are located in the large pocket area according to the structure model of *Kp*ADH. Consequently, these three variants might have different enzymatic properties due to their different pocket conformations. The stereoselectivity of *Kp*ADH_{M131F}, *Kp*ADH_{S196Y} and *Kp*ADH_{S237A} was 82.1, 74.7 and 96.1%, respectively.

High-throughput characterization of *Kp*ADH mutants

Most importantly, this DNPH method could also be applied in the high-throughput characterization of carbonyl reductases. Introduction of different mutations and the diversity in natural biocatalysts might confer different catalytic properties. However, traditional characterization of substrate profiles is highly dependent on the HPLC/GC analysis, and time and labour consuming. Many potential mutants and naturally evolved biocatalysts might be missed due to the incomprehensive characterization of the candidates developed by protein engineering or genome data mining. To fully recognize the potential of these variants in the asymmetric reduction of prochiral ketones, we attempted to use the DNPH method in high-throughput characterization of the variants. About twenty prochiral ketone substrates, including

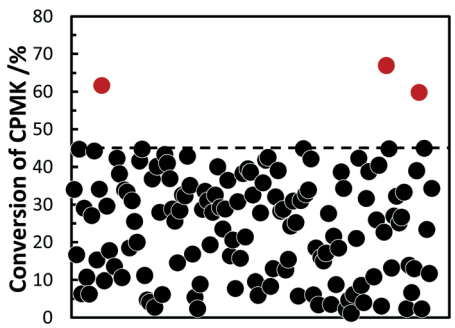

Fig. 3 High-throughput screening of the random mutagenesis library of *Kp*ADH. Red dots refer to the selected mutants. Dashed line denotes the conversion of wild type *Kp*ADH.

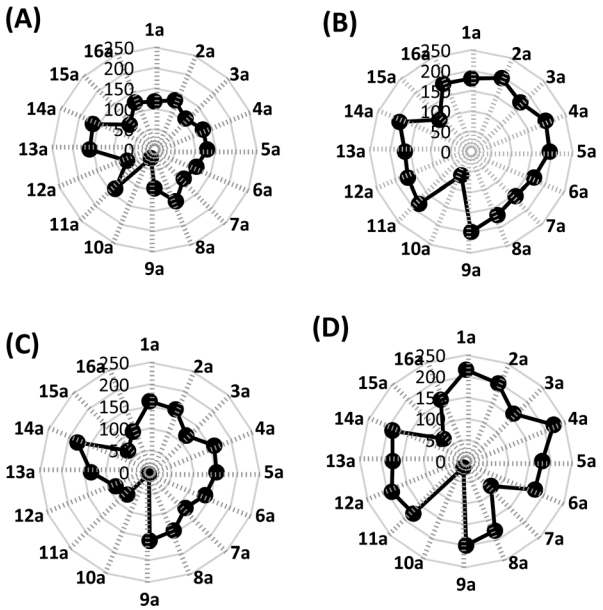

Fig. 4 Substrate profiles of *Kp*ADH and variants toward diaromatic ketones (**1a**–**7a**), aromatic ketones (**8a**–**11a**) and aliphatic ketones/diketones (**12a**–**16a**). (A) *Kp*ADH; (B) *Kp*ADH_{M131F}; (C) *Kp*ADH_{S196Y}; (D) *Kp*ADH_{S237A}. Specific activities (U mg^{-1} wet whole cells) are shown in the radar scheme (●). For details, see Table S2 in the ESI.†

keto-acids, keto-esters, aliphatic ketones/diketones, aromatic ketones and diaromatic ketones, were examined for colorimetric reaction with DNPHzine, and the absorbance spectra of their corresponding DNPHzone are illustrated in Fig. S8–S23.† However, no red-brown color and no obvious absorbance peak were detected with keto-acids and keto-esters. For keto-esters, delocalization in the molecules would happen when a lone-pair of electrons interacts with the ρ-orbital of the carbonyl carbon, and the resonance associated stability would be lost by addition of a functional reagent for the carbonyl group. As a result, these compounds are more resistant to the reactions, showing no remarkable color change.[28] For keto-acids, the negatively charged carboxylic groups may be nucleophilically attacked by DNPHzine. Distinct absorbance peaks were obtained with aliphatic ketones/diketones, aromatic ketones and diaromatic ketones, especially for diketones (**13a**–**16a**) due to the diketone groups. The calibration curves of sixteen prochiral ketones (Scheme 1) were determined for further quantification (see the ESI†).

Substrate profiles of *Kp*ADH and variants toward these ketones were high-throughput assayed in 96-well plates using recombinant whole cells. The specific activities and conversion are shown in Fig. 4 and Tables S1 and S2.† After 6 h, the

Table 3 Kinetic parameters of *Kp*ADH and variants

Enzyme	K_m [mM]	k_{cat} [s^{-1}]	k_{cat}/K_m [s^{-1} mM^{-1}]	ee [%]
*Kp*ADH	0.86 ± 0.04	14.4 ± 0.6	16.8	82.0
KpADH_{M131F}	1.18 ± 0.22	20.9 ± 1.5	17.8	82.1
KpADH_{S196Y}	0.94 ± 0.08	18.2 ± 0.9	19.3	74.7
KpADH_{S237A}	0.28 ± 0.05	22.2 ± 1.0	79.2	96.1

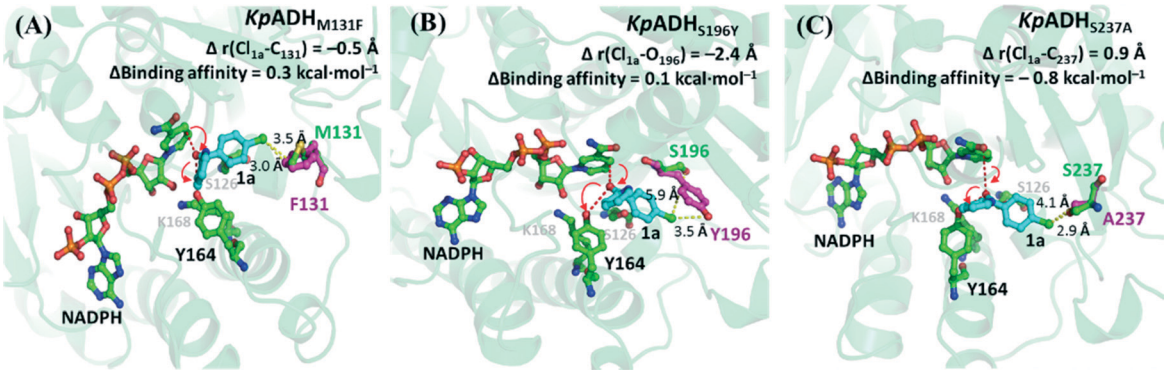

Fig. 5 Molecular docking results of substrate **1a** in *Kp*ADH$_{M131F}$ (A), *Kp*ADH$_{S196Y}$ (B) and *Kp*ADH$_{S237A}$ (C). Catalytic triad, NADPH and wild-type sites are displayed in green, mutated sites are shown in purple, and the docked **1a** is illustrated in cyan. The distances between Cl of **1a** and C of 131 site, O of 196 site and C of 237 site are illustrated in yellow dashed lines. Hydride transfer is shown by red dashed lines and arrows.

reaction was stopped and the conversion was determined by the DNPH method. All the tested prochiral ketones could be reduced, with varied efficiency. *Kp*ADH$_{M131F}$ and *Kp*ADH$_{S237A}$ exhibit higher conversion toward diaryl ketones than *Kp*ADH and *Kp*ADH$_{S196Y}$. *Kp*ADH$_{S237A}$ displays the highest conversion (87.6%) in the asymmetric reduction of S1, 40% higher than that of *Kp*ADH. With regard to the specific activity which was determined by controlling the reaction progress within <10% conversion, all three variants display higher activity toward the tested ketones compared with *Kp*ADH. The specific activities of *Kp*ADH$_{M131F}$, *Kp*ADH$_{S196Y}$ and *Kp*ADH$_{S237A}$ toward **1a** are 0.18, 0.16 and 0.22 U mg^{-1} wet whole cells, which are 1.5, 1.3 and 1.8 folds of *Kp*ADH, respectively. Variants *Kp*ADH$_{M131F}$ and *Kp*ADH$_{S237A}$ show a higher substrate preference toward diaromatic ketones. The substrate specificity analysis could provide guidance for the application of *Kp*ADH variants in the preparation of optically active secondary alcohols.

Kinetics and molecular docking of *Kp*ADH mutants

To obtain insight into the potential mechanisms of the improved variants, kinetics and molecular docking analyses were performed. Variants *Kp*ADH, *Kp*ADH$_{M131F}$, *Kp*ADH$_{S196Y}$ and *Kp*ADH$_{S237A}$ were purified to homogeneity as shown in Fig. S3–S6† at 300 mM imidazole. The K_m and k_{cat}/K_m of *Kp*ADH are 0.86 mM and 16.8 s^{-1} mM^{-1}. The K_m values of *Kp*ADH$_{M131F}$ and *Kp*ADH$_{S196Y}$ are 1.18 mM and 0.94 mM, higher than that of *Kp*ADH, indicating their weaker affinity toward **1a** (Table 3). *Kp*ADH$_{S237A}$ displays the lowest K_m (0.28 mM) and the highest k_{cat}/K_m (79.2 s^{-1} mM^{-1}) among *Kp*ADH and the three variants. The homology structure of *Kp*ADH was constructed and shown in Fig. S7† using the crystal structure of yeast methylglyoxal/isovaleraldehyde reductase in complex with NADP$^+$ (PDB: 4PVD) as the template. Substrate **1a** was docked into the active center of *Kp*ADH, *Kp*ADH$_{M131F}$, *Kp*ADH$_{S196Y}$ and *Kp*ADH$_{S237A}$ using Autodock Vina. The distance between **1a** and the mutation sites, as well as the binding affinity were calculated and illustrated in Fig. 5. The active center consists of small and large pockets for substrate binding. Since the 4-chlorophenyl group is a little larger than the pyrid-2-yl group of **1a**, the 4-chlorophenyl group is docked into the large substrate binding pocket. The hydride transfer from NADPH to the prochiral carbonyl group results in (*R*)-CPMA (Fig. 5). M131, S196 and S237 all belong to the large pocket. Mutation on these sites produced different effects on the binding and catalysis of **1a**. In *Kp*ADH$_{M131F}$ and *Kp*ADH$_{S196Y}$, mutations F131 and Y196 render the large substrate binding pocket smaller, and the size difference between the large and small binding pockets is reduced. Therefore, the pyrid-2-yl group could be docked into the large binding pocket instead of the small one. As illustrated in molecular docking, a reduced distance difference (Δr) and higher binding affinity (ΔBinding affinity) between **1a** and 131/196 sites were observed (Fig. 5(A) and (B)). As expected, the K_m of *Kp*ADH$_{M131F}$ and *Kp*ADH$_{S196Y}$ were increased and the ee values were decreased compared with those of *Kp*ADH (Table 3). In *Kp*ADH$_{S237A}$, the large binding pocket was enlarged, due to the mutation of serine into smaller alanine. In comparison with *Kp*ADH, the distance between **1a** and A237 was increased by 0.9 Å, while the binding affinity was decreased by 0.8 kcal mol^{-1}. It is presumed that the enlarged large binding pocket led to an enhanced substrate binding affinity and discrimination between 4-chlorophenyl and pyrid-2-yl groups of **1a**. Consequently, the k_m of *Kp*ADH$_{S237A}$ was reduced to 0.28 mM, while the k_{cat}/K_m was 79.2 s^{-1} mM^{-1}, representing 4.71-fold of *Kp*ADH. Most importantly, the ee of *Kp*ADH$_{S237A}$ also increased to 96.1% (*R*). Our results suggest that steric hindrance plays an important role in the substrate binding and conversion of *Kp*ADH.

Conclusions

In summary, we have developed a sensitive colorimetric method that enables facile high-throughput screening and characterization of carbonyl reductases. Especially, this DNPH method displays promising potential in the activity assay of a whole-cell system. Three variants of *Kp*ADH with improved activity toward CPMK were identified from a random mutagenesis library employing this method. The catalytic

performance of *Kp*ADH and its variants in the asymmetric reduction of sixteen prochiral ketones was high-throughput characterized and could be regarded as guidance in the further application potential of these variants. Also, kinetics and molecular docking analyses of *Kp*ADH variants were conducted to understand their catalytic and enantioselective mechanisms.

Acknowledgements

We are grateful to the National Natural Science Foundation of China (21276112, 21506073), the Natural Science Foundation of Jiangsu Province (BK20150003), the Fundamental Research Funds for the Central Universities (JUSRP51409B), the Program of Introducing Talents of Discipline to Universities (111-2-06), and a project funded by the Priority Academic Program Development of Jiangsu Higher Education Institutions for the financial support of this research.

Notes and references

1 A. Schmid, J. S. Dordick, B. Hauer, A. Kiener, M. Wubbolts and B. Witholt, *Nature*, 2001, **409**, 258–268.
2 Y. Ni, J. Y. Zhou and Z. H. Sun, *Process Biochem.*, 2012, **47**, 1042–1048.
3 H. Frank and M. Edmund, Enzyme Assays: High-throughput Screening, *Genetic Selection and Fingerprinting*, 2007, vol. 39, pp. 77–93.
4 G. C. Xu and Y. Ni, *Bioresour. Bioprocess.*, 2015, **2**, 15.
5 T. Davids, M. Schmidt, D. Böttcher and U. T. Bornscheuer, *Curr. Opin. Chem. Biol.*, 2013, **17**, 215–220.
6 C. A. Denard, H. Q. Ren and H. M. Zhao, *Curr. Opin. Chem. Biol.*, 2015, **25**, 55–64.
7 W. S. Liu and R. R. Jiang, *Appl. Microbiol. Biotechnol.*, 2015, **99**, 2093–2104.
8 T. W. Johannes, R. D. Woodyer and H. M. Zhao, Enzyme Assays: High-throughput Screening, *Genetic Selection and Fingerprinting*, 2006.
9 F. Shi, J. Tan, J. Chua, Y. H. Wang, Y. P. Zhuang and S. L. Zhang, *J. Microbiol. Methods*, 2015, **109**, 134–139.
10 T. Nakai, S. Morikawa, N. Kizaki and Y. Yasohara, *Eur. Pat.*, 2001, 1416050 A1.
11 Y. C. He, D. P. Zhang, Z. C. Tao, X. Zhang and Z. X. Yang, *Bioresour. Technol.*, 2014, **172**, 342–348.
12 M. C. Forchin, M. Crotti, F. G. Gatti, F. Parmeggiani, E. Brenna and D. Monti, *ChemBioChem*, 2015, **16**, 1571–1573.
13 J. Zhao, T. Kardashliev, A. J. Ruff, M. Bocola and U. Schwaneberg, *Biotechnol. Bioeng.*, 2015, **111**, 2380–2389.
14 G. Hill and J. H. Brady, *Analyst*, 1926, **51**, 77–78.
15 W. L. Wang, G. L. Li, Z. Y. Ji, N. Hu and J. M. You, *Food Anal. Methods*, 2014, **7**, 1546–1556.
16 A. Ahmed, J. Reda, J. Schnelle-Kreis, G. Orasche, J. Abbaszade and J. M. Lintelmann, *Atmos. Environ.*, 2015, **112**, 370–380.
17 Y. P. Xue, W. Wang, Y. J. Wang, Z. Q. Liu, Y. G. Zheng and Y. C. Shen, *Bioprocess Biosyst. Eng.*, 2012, **35**, 1515–1522.
18 P. Stocker, E. Ricquebourg, N. Vidal, C. Villard, D. Lafitte, L. Sellami and S. Pietri, *Anal. Biochem.*, 2015, **482**, 55–61.
19 G. C. Xu, L. L. Zhang and Y. Ni, *J. Biotechnol.*, 2016, **222**, 29–37.
20 H. Lineweaver and D. Burk, *J. Am. Chem. Soc.*, 1934, **25**, 658–666.
21 P. C. Guo, Z. Z. Bao, X. X. Ma, Q. Xia and W. F. Li, *Biochim. Biophys. Acta, Bioenerg.*, 2014, **1844**, 1486–1492.
22 O. Trott and A. J. Olson, *J. Comput. Chem.*, 2010, **31**, 455–461.
23 G. Moroff, R. S. Ochs and K. G. Brandt, *Arch. Biochem. Biophys.*, 1976, **173**, 42–49.
24 G. L. Long and J. D. Winefordner, *Anal. Chem.*, 1983, **55**, 712A–724A.
25 P. J. Benesty, J. Chen, Y. Huang and I. Cohen, *Springer Topics in Signal Processing*, 2009, vol. 2, pp. 1–4.
26 J. R. Sauer and B. K. Williams, *J. Wildl. Manage.*, 1989, **53**, 137–142.
27 A. Nobili, Y. F. Tao, I. V. Pavlidis, T. Bergh, H. J. Joosten, T. W. Tan and U. T. Bornscheuer, *ChemBioChem*, 2015, **16**, 805–810.
28 J. W. Thorpe and J. Warkentin, *Can. J. Chem.*, 1973, **51**, 927–935.